JOURNAL OF GUIDANCE, CONTROL, AND DYNAMICS
Vol. 19, No. 1, January–February 1996

Finite Difference Scheme for Automatic Costate Calculation

Hans Seywald* and Renjith R. Kumar†
Analytical Mechanics Associates, Inc., Hampton, Virginia 23665

A method for the automatic calculation of costates using only results obtained from direct optimization techniques is presented. The approach is based on finite differences and exploits the relation between the costates and certain sensitivities of the cost function. The complete theory for treating free, control constrained, interior-point constrained, and state constrained optimal control problems is presented. An important advantage of the method presented here is that it does not require a priori identification of the optimal switching structure. As a numerical example, a state constrained version of the Brachistochrone problem is solved, and the results are compared to the optimal solution obtained from Pontryagin's minimum principle. The agreement is found to be excellent.

I. Introduction

THE methods of solution for optimal control problems are divided into two major classes, namely, the direct methods and the indirect methods. The indirect methods are based on Pontryagin's minimum principle[1–5] and require the numerical solution of multipoint boundary value problems (MPBVPs).[6–8] The advantages of these methods lie in their fast convergence in the neighborhood of the optimal solution, even if the cost gradients are very shallow. Furthermore, the optimal solutions are obtained with extremely high precision, and subtle properties of the optimal solution can be clearly identified. On the other hand, indirect optimization techniques usually require excellent initial guesses before convergence can be achieved at all. This requirement is especially restrictive as these methods involve Lagrange multipliers whose physical meaning is nonintuitive and provides little help for generating reasonable initial guesses on an ad hoc basis. Furthermore, the switching structure, that is, the sequence in which different control logics become active along the optimal solution, has to be guessed in advance.

Direct optimization techniques rely on restricting the infinite dimensional space of admissible candidate trajectories to a finite dimensional subspace of the original function space.[9] The optimal solution within this subspace is then determined by directly optimizing the cost criterion through nonlinear programming.[10] The convergence radius of such methods is usually much larger than that of indirect methods. Furthermore, initial guesses have to be provided only for physically intuitive quantities, such as states and, possibly, controls. Finally, the switching structure of the optimal solution need not be guessed at all.

In an attempt to get the best of both worlds, the present paper introduces the theoretical background for a finite difference based scheme to approximately calculate the costates associated with optimal control problems. Most of the results presented here are well known and documented, for example, in Bryson and Ho.[2] But the derivation given here and some results obtained for constrained optimal control problems provide additional insights and open the door for numerical applications.

Numerically, the methods presented here require the calculation of approximate optimal trajectories subject to the reference boundary conditions and subject to certain perturbed boundary conditions. There are no restrictions or special requirements on the method used to generate the suboptimal solutions, so that the methods presented in this paper can be basically paired with any existing direct optimization scheme.

As a numerical example, a state constrained version of the Brachistochrone problem[2] is treated, and the results are compared to the optimal solution obtained from Pontryagin's minimum principle.

Other methods for automatic costate calculation are discussed, for example, in Refs. 12–14. In Ref. 12 the final costate values associated with the prescribed boundary conditions are integrated backwards along the frozen solution obtained through direct optimization. This approach requires the explicit implementation of the costate dynamics. In Ref. 13 a best match discretized costate function of time associated with the frozen trajectory obtained through direct optimization is obtained by minimizing a least squares error comprising the transversality conditions and discretized costate dynamics. The linearity of the costate dynamics and the transversality conditions makes this method noniterative. In Ref. 14 a relation between the discrete NLP multipliers and the time-varying Lagrange multipliers is derived and exploited for automatic costate calculation.

II. Unconstrained Optimal Control Problems

A. Problem Formulation

Let us consider the following optimal control problem stated in Mayer form:

$$\min_{u \in (PWC[t_0,t_f])^m} J[u], \qquad J[u] = \phi[x(t_f), t_f] \tag{1}$$

subject to the conditions

$$\dot{x}(t) = f[x(t), u(t)] \tag{2}$$

$$\theta[x(t_0), t_0] = 0 \tag{3}$$

$$\psi[x(t_f), t_f] = 0 \tag{4}$$

Here, $t \in \boldsymbol{R}$, $x(t) \in \boldsymbol{R}^n$, and $u(t) \in \boldsymbol{R}^m$ are time, state vector, and control vector, respectively. The functions, ϕ: $\boldsymbol{R}^{n+1} \to \boldsymbol{R}$, f: $\boldsymbol{R}^{n+m} \to \boldsymbol{R}^n$, θ: $\boldsymbol{R}^{n+1} \to \boldsymbol{R}^{s_0}$, $s_0 \leq n+1$, and ψ: $\boldsymbol{R}^{n+1} \to \boldsymbol{R}^{s_f}$, $s_f \leq n$, are assumed to be sufficiently smooth with respect to their arguments of whatever order is required in this paper. $(PWC[t_0, t_f])^m$ denotes the set of all piecewise continuous functions defined on the interval $[t_0, t_f]$ into $\boldsymbol{R}^m$. Conditions (2–4) represent the differential equations of the underlying dynamical system, the initial conditions, and the final conditions, respectively.

Note that no control constraints, interior-point constraints, or state constraints are considered in problem (1–4). Such complicating features are introduced in Secs. III, IV, and V, respectively.

B. Minimum Principle

Let us assume that a solution to problem (1–4) exists. Then, under certain normality and regularity conditions,[1–5] it can be shown that there are constant multiplier vectors $\beta \in \boldsymbol{R}^{s_0}$, $\nu \in \boldsymbol{R}^{s_f}$, and a

Received Aug. 29, 1994; revision received April 20, 1995; accepted for publication June 27, 1995. Copyright © 1995 by the American Institute of Aeronautics and Astronautics, Inc. All rights reserved.

*Supervising Engineer, 17 Research Drive, working under contract at Guidance and Controls Branch, NASA Langley Research Center, Hampton, VA 23681. Member AIAA.

†Senior Engineer, working under contract at Space Systems and Concepts Division, NASA Langley Research Center, Hampton, VA 23681. Member AIAA.

time-varying multiplier vector $\lambda(t) \in \boldsymbol{R}^n$ which is nonzero for all times $t \in [t_0, t_f]$ such that

$$\dot{\lambda}^T = -\frac{\partial H}{\partial x} \tag{5}$$

$$\lambda(t_0)^T = -\beta^T \frac{\partial \theta}{\partial x(t_0)} \tag{6}$$

$$\lambda(t_f)^T = \frac{\partial \phi}{\partial x(t_f)} + \nu^T \frac{\partial \psi}{\partial x(t_f)} \tag{7}$$

$$H[x(t_0), \lambda(t_0), u(t_0)] = \beta^T \frac{\partial \theta}{\partial t_0} \tag{8}$$

$$H[x(t_f), \lambda(t_f), u(t_f)] = -\frac{\partial \phi}{\partial t_f} - \nu^T \frac{\partial \psi}{\partial t_f} \tag{9}$$

where

$$H(x, \lambda, u) := \lambda^T f(x, u) \tag{10}$$

denotes the Hamiltonian. At each instant of time the optimal control u^* satisfies the Pontryagin minimum principle

$$u^* = \arg \min_{u \in \boldsymbol{R}^m} H(x, \lambda, u) \tag{11}$$

By virtue of the assumed smoothness of $f(x, u)$ Eq. (11) implies

$$\left. \frac{\partial H}{\partial u} \right|_{u^*} = 0 \tag{12}$$

$$\delta u^T \left. \frac{\partial^2 H}{\partial u^2} \right|_{u^*} \delta u \geq 0 \qquad \forall\, \delta u \in \boldsymbol{R}^m \tag{13}$$

C. Augmented Cost Function

In optimal control it is a standard procedure to construct an augmented cost function by linking expressions to the original cost function that have to be zero along the optimal solution.[2] Necessary conditions for optimality are then obtained from the condition that the first variation of the augmented cost function be equal zero. This step is justified by a generalized multiplier theorem, which is, loosely speaking, an infinite dimensional version of the Kuhn–Tucker conditions.[9]

In the sections to follow, we will derive expressions for the sensitivity of the cost function with respect to perturbations in the initial time and the initial states. To obtain expressions for these sensitivities in terms of the costates associated with the optimal reference solution, we formally repeat the analysis of augmenting the cost function and expanding it about the reference solution, as is usually done to derive the first-order necessary conditions of optimal control. We consider, however, the Lagrange multipliers as a priori fixed and equal to the multipliers associated with the optimal solution. This approach leads to expressions for the sensitivities of the augmented cost function in terms of the Lagrange multipliers. An approximate numerical calculation of these sensitivities through finite differences is then based on the observation that all penalty terms in the augmented cost function are zero along the numerically generated reference solution, i.e., that the Lagrange multipliers can be expressed in terms of sensitivities of the original cost function.

D. Relation Between the Lagrange Multipliers $\boldsymbol{\lambda}(t)$ and Cost Sensitivities

Let us define the following augmented cost function:

$$\bar{J} = \phi[x(t_f), t_f] + \nu^{*T} \psi[x(t_f), t_f] + \int_{t_0}^{t_f} \{\lambda^{*T}[f(x, u) - \dot{x}]\}\, dt \tag{14}$$

Note that the term $\beta^T \theta[x(t_0), t_0]$ has not been included. Here and in the following, the superscript asterisk denotes quantities associated with the optimal solution to problem (1–4), also called the reference solution. Furthermore, let superscript p denote quantities associated with optimal solutions to problem (1), (2), and (4) with initial conditions prescribing the states and the time at values slightly perturbed with respect to the values obtained for the reference solution. If we consider such perturbations parameterized by, say, a scalar ϵ, and expand quantities associated with the perturbed solution into a Taylor series about $\epsilon = 0$, e.g., $u^p(t, \epsilon) = u^*(t) + \epsilon \cdot \delta u(t) + \mathcal{O}^2$, with

$$\delta u(t) = \left. \frac{du^p(t, \epsilon)}{d\epsilon} \right|_{\epsilon = 0}$$

then the first-order terms satisfy

$$\begin{aligned} \delta u(t) &= u^p(t) - u^*(t) + \mathcal{O}^2, & \delta x(t) &= x^p(t) - x^*(t) + \mathcal{O}^2 \\ dt_0 &= t_0^p - t_0^* + \mathcal{O}^2, & dt_f &= t_f^p - t_f^* + \mathcal{O}^2 \\ dx_0 &= x_0^p - x_0^* + \mathcal{O}^2, & dx_f &= x_f^p - x_f^* + \mathcal{O}^2 \end{aligned} \tag{15}$$

and are called (first) variations. Here and in the following, $\mathcal{O}^2$ stands for terms of order ϵ^2 and higher. The first variation of the augmented cost function $\bar{J}$ defined in Eq. (14) satisfies $d\bar{J} = \bar{J}^p - \bar{J}^* + \mathcal{O}^2$ and can be written in the form

$$d\bar{J} = (\phi + \nu^T \psi)_x\, dx_f + (\phi + \nu^T \psi)_t\, dt_f + \int_{t_0}^{t_f} \left[H_x \delta x + H_u \delta u - \lambda^T \delta \dot{x} \right] dt \tag{16}$$

All states, costates, and controls on the right-hand side of Eq. (16) are evaluated along the optimal solution to problem (1–4) and the superscript asterisks are dropped for convenience. Using

$$\begin{aligned} \int_a^b -\lambda^T \delta \dot{x}\, dt &= -\lambda^T \delta x |_a^b + \int_a^b \dot{\lambda}^T \delta x\, dt \\ &= -\lambda^T dx|_a^b + \lambda^T \dot{x}\, dt|_a^b + \int_a^b \dot{\lambda}^T \delta x\, dt + \mathcal{O}^2 \\ &= -\lambda^T dx|_a^b + H\, dt|_a^b + \int_a^b \dot{\lambda}^T \delta x\, dt + \mathcal{O}^2 \end{aligned} \tag{17}$$

to eliminate the $\delta \dot{x}$-term yields, after rearranging and dropping the $\mathcal{O}^2$ terms

$$\begin{aligned} d\bar{J} = {} & \lambda(t_0)^T dx_0 - H|_{t_0} dt_0 + \left[(\phi + \nu^T \psi)_x - \lambda(t_f)^T \right] dx_f \\ & + \left[(\phi + \nu^T \psi)_t + H|_{t_f} \right] dt_f \\ & + \int_{t_0}^{t_f} \left(H_x + \dot{\lambda}^T \right) \delta x + (H_u) \delta u\, dt \end{aligned} \tag{18}$$

By virtue of Eqs. (5), (7), (9), and (12), the coefficients of dx_f, dt_f, and all terms under the integral in Eq. (18) vanish, and we arrive at

$$d\bar{J} = \lambda(t_0)^T dx_0 - H|_{t_0} dt_0 \tag{19}$$

It is clear that the value of the augmented cost function (14) is equal to the value of the original cost function (1) as long as the state equations (2) and the terminal conditions (4) are satisfied. Hence, if the perturbed quantities $x^p(t)$, $u^p(t)$, represent a solution to the dynamical system (2) and the boundary conditions (4), the right-hand side of Eq. (19) provides an expression for the sensitivity of the original cost function (1) with respect to perturbations in the initial time and the initial states, i.e.,

$$dJ = \lambda(t_0)^T dx_0 - H|_{t_0} dt_0 \tag{20}$$

Note that the symbols λ, t_0, and H denote quantities associated with the optimal reference solution, and the superscript asterisks are dropped only for convenience.

In the following sections we will show how Eq. (20) can be used to approximately determine the unknown Lagrange multipliers $\lambda(t_0)$ if only a method is available to generate reasonably precise approximations to the reference solution and to the perturbed solutions, respectively. Note that the left-hand side of Eq. (20) can be approximated by $J^p - J$, if only the perturbations used to generate J^p are sufficiently small.

E. Numerical Calculation of $\lambda(t_0)$

We first present a method for generating a family of perturbed solutions, each one of which can be used to calculate the left-hand side of Eq. (20) numerically through finite differences. The quantity $n+1$ such perturbed solutions (n is the dimension of the state vector $\boldsymbol{x}$) can be obtained by resolving the optimal control problem (1–4) with the initial conditions (3) deleted and replaced by $n+1$ explicit conditions on the initial time t_0 and the initial state x_0. Explicitly, let the ith perturbed solution, denoted by superscript i, be obtained by solving problem (1), (2), and (4), subject to the initial conditions

$$\begin{aligned} x^i\left(t_0^i\right) &= x^*\left(t_0^*\right) + \Delta x_0^i \\ t_0^i &= t_0^* + \Delta t_0^i \end{aligned} \tag{21}$$

Here, the jth component $(\Delta x_0^i)_j$ of the n-dimensional perturbation vector $\Delta \boldsymbol{x}_0^i$ is given by

$$\left(\Delta x_0^i\right)_j = \epsilon^i \delta_{i,j}, \qquad j = 1, \ldots, n \tag{22}$$

and the perturbation in initial time is given by

$$\Delta t_0^i = \epsilon^i \delta_{i,n+1} \tag{23}$$

Here, the ϵ^i, $i = 1, \ldots, n+1$, are user chosen small nonzero quantities and $\delta_{i,j}$ denotes the Kronecker symbol defined by

$$\delta_{i,j} = \begin{cases} 1 & \text{if} \quad i = j \\ 0 & \text{if} \quad i \neq j \end{cases} \tag{24}$$

For each of the $n+1$ pairs consisting of one of the perturbed solutions and the reference solution, the left-hand side of Eq. (20) is evaluated approximately through finite differences. Through Eq. (20), this yields $n+1$ conditions in the $n+1$ unknowns $\lambda(t_0) \in \boldsymbol{R}^n$ and $H|_{t_0} \in \boldsymbol{R}$. Concisely, these conditions can be written in the form

$$\boldsymbol{D}\boldsymbol{J}^T = \boldsymbol{G}^T \cdot \boldsymbol{P}^T \tag{25}$$

where

$$\boldsymbol{D}\boldsymbol{J}^T = [\mathrm{d}J^1, \ldots, \mathrm{d}J^{n+1}] \tag{26}$$

denotes the vector of the numerically calculated variations in the cost function,

$$\boldsymbol{G}^T = \left[\lambda^T|_{t_0}, -H|_{t_0}\right]\Big|_* \tag{27}$$

is the vector of unknowns (again, note that the symbols λ, t_0, and H denote quantities associated with the optimal reference solution, and that the superscript asterisks are dropped only for convenience), and

$$P^T = \begin{bmatrix} \mathrm{d}x_0^1 & \cdots & \mathrm{d}x_0^{n+1} \\ \mathrm{d}t_0^1 & \cdots & \mathrm{d}t_0^{n+1} \end{bmatrix} \tag{28}$$

is an $(n+1) \times (n+1)$ matrix whose ith column consists of the perturbations in initial states and time associated with the ith perturbed solution.

If the perturbation matrix (28) is nonsingular then Eq. (25) can be solved for G and we obtain

$$G = P^{-1} \cdot DJ \tag{29}$$

For the perturbations (22) and (23) P takes the form of a diagonal matrix with the nonzero displacements ϵ_i as the diagonal elements, so that P is guaranteed to be nonsingular.

F. Numerical Calculation of $\lambda(t)$ for $t > t_0^*$

The ideas presented in Secs. II.D and II.E to calculate $\lambda^*(t_0^*)$ can be easily extended to the calculation of $\lambda^*(t_1)$ for any time t_1 with $t_0^* < t_1 < t_f^*$. Loosely speaking, we consider t_1 as the new initial time. Explicitly, a new reference solution, again denoted by superscript asterisk, is defined by restricting the original reference solution to the time domain $[t_1, t_f^*]$, and $n+1$ perturbed solutions are obtained by solving problem (1), (2), and (4), subject to the initial conditions

$$\begin{aligned} x^i\left(t_0^i\right) &= x^*(t_1) + \Delta x_1^i \\ t_0^i &= t_1 + \Delta t_1^i \end{aligned} \tag{30}$$

In complete analogy to the preceding section, this leads to the relation (29), however, with G defined in Eq. (27) evaluated at t_1 rather than at t_0^*, and with P defined in Eq. (28) consisting of the perturbations $\mathrm{d}x_1$, $\mathrm{d}t_1$, rather than $\mathrm{d}x_0$, $\mathrm{d}t_0$.

A numerically inexpensive way of generating perturbed solutions for initial time $t_1 > t_0^*$ is to reuse the perturbed solutions generated for initial time t_0^* and to restrict these solutions to the time interval $[t_1 + \Delta t_1^i, t_f^*]$. The restricted trajectories can be considered solutions to problem (1), (2), and (4), with the initial conditions (30) for appropriately chosen Δx_1^i and Δt_1^i. These perturbations are dictated now by the natural evolution of the respective perturbed solutions obtained for the time interval $[t_0^*, t_f^*]$. The associated matrix P is guaranteed to be analytically nonsingular as long as the reference solution satisfies the no-conjugate-point condition on the interval $[t_0^*, t_f^*]$ (Refs. 2 and 15). However, the condition number of matrix P can still become so large that P becomes numerically singular. In this case new perturbation trajectories have to be calculated on the basis of Eq. (30) for hand-picked perturbations Δx_1^i, Δt_1^i in the style of Sec. II.E.

G. Calculation of $\lambda(t_f)$

The calculation of $\lambda(t)$ as described in the preceding two sections becomes increasingly difficult as t approaches t_f^*. Equation (29) used for calculating $\lambda(t)$ is based, loosely speaking, on linearizing the augmented cost function (14) about the asterisk-indicated reference solution. Numerically, the approach relies on applying sufficiently small perturbations on the reference solution such that the dependence of all changes on the magnitude of the perturbations ϵ^i introduced in Eqs. (22) and (23) is close to linear. To achieve good performance, the size of the perturbations has to be reduced as t approaches t_f, and, at $t = t_f$ the method based on Eq. (29) breaks down altogether.

To calculate the costates at $t = t_f$, we can resort to Eq. (7), if only the constant multiplier vector $\boldsymbol{\nu} \in \boldsymbol{R}^{s_f}$ is known. The method for calculating $\boldsymbol{\nu}$ is only described briefly, here. A similar method for calculating the multipliers associated with interior-point constraints is treated in more detail in Sec. V.D.

To calculate the multiplier vector $\boldsymbol{\nu}$ associated with problem (1–4) the original state vector x is first augmented by an s_f-dimensional state vector $\boldsymbol{a}$ through the dummy equations $\dot{a} = 0$ and $\boldsymbol{a}(t_0) = 0$. Then the boundary conditions (4) are changed to $\psi[x(t_f), t_f] - \boldsymbol{a}(t_f) = 0$. It can be verified easily that the solution to this augmented optimal control problem is identical to the solution of the original problem (1–4) [identical in $x(t)$, $\lambda(t)$, $u(t)$, t_0, t_f, β, and $\boldsymbol{\nu}$]. Furthermore, it can be verified analytically that $\lambda_a(t)$ is identically constant with the value $\lambda_a(t) = -\boldsymbol{\nu}$. Through the methods discussed in Sec. II.E $\lambda_a(t_0)$ and, hence $\boldsymbol{\nu}$, can be calculated. Then $\lambda(t_f)$ can be determined from Eq. (7).

III. Control Constrained Problems

A. Problem Formulation and Optimality Conditions

For simplicity, let us only consider a single scalar control inequality constraint. The generalization to vector-valued constraints and to equality constraints is then straightforward. Note that, with respect to control equality constraints, control inequality constraints have the added difficulty that the optimal switching structure is not known in advance.

Explicitly, consider problem (1–4) subject to the constraint

$$c(x, u, t) \le 0 \tag{31}$$

Along subarcs of the optimal solution where control constraint (31) is satisfied with strict inequality, the optimality conditions presented in Eqs. (5–13) are satisfied and the solution behaves as if the constraint (31) were deleted. Along subarcs, say, $[t_1, t_2]$, throughout which $c(x, u, t) = 0$, the minimum principle[1–5] takes the form

$$u^* = \arg \min_{u \in R^m, c(x,u,t)=0} H \tag{32}$$

where H denotes the Hamiltonian defined in Eq. (10). Then, at each instant of time along the time interval $[t_1, t_2]$, the Kuhn–Tucker conditions

$$\left.\left(\frac{\partial H}{\partial u} + \mu \frac{\partial c}{\partial u}\right)\right|_{u^*} = 0 \tag{33}$$

$$c(x, u, t)|_{u^*} = 0 \tag{34}$$

$$\Delta u^T \left.\left(\frac{\partial^2 H}{\partial u^2} + \mu \frac{\partial^2 c}{\partial u^2}\right)\right|_{u^*} \Delta u \geq 0$$

$$\text{for all} \quad \Delta u \in R^m \quad \text{with} \quad \left.\frac{\partial c}{\partial u}\right|_{u^*} \Delta u = 0 \tag{35}$$

yield the values of the optimal control u^* and the scalar multiplier μ, and the evolution of the Lagrange multipliers λ is governed by

$$\dot{\lambda} = -\frac{\partial H}{\partial x} - \mu \frac{\partial c}{\partial x} \tag{36}$$

At both switching times, t_1 and t_2, the Lagrange multipliers λ and the Hamiltonian H are continuous.

B. Relation Between the Lagrange Multipliers $\lambda(t)$ and Cost Sensitivities

Assume we have an optimal solution to problem (1–4) and (31) with the switching structure

$$c(x, u, t) \begin{cases} <0 & \text{on} \quad [t_0, t_1) \\ =0 & \text{on} \quad [t_1, t_2] \\ <0 & \text{on} \quad (t_2, t_f] \end{cases} \tag{37}$$

Consider the augmented cost function

$$\bar{J} = \phi[x(t_f), t_f] + \nu^{*T} \psi[x(t_f), t_f]$$
$$+ \int_{t_0}^{t_f} \{\lambda^{*T}[f(x, u) - \dot{x}] + \mu^{*T} c(x, u, t)\} \, dt \tag{38}$$

where ν^*, $\lambda^*(t)$, and $\mu^*(t)$ denote the constant and time varying multipliers associated with the optimal solution to problem (1–4) and (31). These quantities are fixed in the following analysis. Repeating the analysis presented in Sec. II.D, i.e., expanding the augmented cost function about the asterisk indicated reference solution, and using Eq. (17) to eliminate the $\delta\dot{x}$ term, we arrive at the following expression for the first variation of the augmented cost function (38):

$$\mathrm{d}\bar{J} = \left[(\phi + \nu^T \psi)_x - \lambda(t_f)\right] \mathrm{d}x_f + \left[(\phi + \nu^T \psi)_t + H|_{t_f}\right] \mathrm{d}t_f$$
$$+ \int_{t_0}^{t_1} \left[\left(H_x + \mu c_x + \dot{\lambda}^T\right)\delta x + (H_u + \mu c_u)\delta u\right] \mathrm{d}t$$
$$+ \int_{t_1}^{t_2} \cdots \, \mathrm{d}t + \int_{t_2}^{t_f} \cdots \, \mathrm{d}t + \left(\lambda^T|_{t_1^+} - \lambda^T|_{t_1^-}\right) \mathrm{d}x_1$$
$$+ \left(\lambda^T|_{t_2^+} - \lambda^T|_{t_2^-}\right) \mathrm{d}x_2 - \left(H|_{t_1^+} - H|_{t_1^-}\right) \mathrm{d}t_1$$
$$- \left(H|_{t_2^+} - H|_{t_2^-}\right) \mathrm{d}t_2 + \lambda^T(t_0) \, \mathrm{d}x_0 - H|_{t_0} \, \mathrm{d}t_0 \tag{39}$$

Note that to perform the integration by parts of the $\delta\dot{x}$ term it is necessary to break the integral $\int_{t_0}^{t_f}$ at the switching times t_1, t_2. Continuity of the integrand across these switching times can not be assumed a priori.

By choice of λ, μ, and ν, we find that all coefficients on the right-hand side, except for those corresponding to $\mathrm{d}x_0$ and $\mathrm{d}t_0$, are zero, and we obtain the same result as in the unconstrained case, namely, $d\bar{J} = \lambda(t_0)^T \, \mathrm{d}x_0 - H|_{t_0} \, \mathrm{d}t_0$, Eq. (19). From arguments identical to those used in Sec. II.D, it follows that the sensitivity of the augmented cost function is equal to the sensitivity of the original cost function, i.e., $\mathrm{d}J = \lambda(t_0)^T \, \mathrm{d}x_0 - H|_{t_0} \, \mathrm{d}t_0$, as stated in Eq. (20). By virtue of the relation $\mathrm{d}J = J^p - J^* + \mathcal{O}^2$, this result shows that the numerical procedure for calculating costate approximations as discussed in Secs. II.E and II.F can be applied without modifications to control constrained problems. Tacitly, it is assumed here that solutions exist to all problems with the initial states and time perturbed as discussed in Sec. II.E. Note that this requires, as a necessary condition, that constraint (31) depends explicitly on the control u, i.e., $\partial c/\partial u \neq 0$ on $[t_1, t_2]$. The state constrained case, where c is independent of control u, will be treated in Sec. V.

IV. Problems with Interior-Point Constraints

A. Problem Formulation and Optimality Conditions

In this section we consider problem (1–4) subject to an interior point constraint of the general form

$$N[x(t_1), t_1] = 0 \tag{40}$$

For simplicity, we assume that N is scalar. The generalization to vector-valued constraints will be obvious.

In addition to the optimality conditions (5–13) stated for unconstrained problems, the interior point constraint (40) causes a discontinuous jump in the Lagrange multipliers $\lambda(t)$ and in the Hamiltonian H at time t_1. Explicitly,

$$\lambda\left(t_1^+\right)^T = \lambda\left(t_1^-\right)^T - l_0 \frac{\partial N[x(t_1), t_1]}{\partial x(t_1)} \tag{41}$$

$$H|_{t_1^+} = H|_{t_1^-} + l_0 \frac{\partial N[x(t_1), t_1]}{\partial t_1} \tag{42}$$

where l_0 is a constant multiplier that compensates for the degree of freedom lost by enforcing the condition (40).

B. Relation Between the Lagrange Multipliers $\lambda(t)$ and Cost Sensitivities

Consider the augmented cost function

$$\bar{J} = \phi[x(t_f), t_f] + \nu^{*T} \psi[x(t_f), t_f]$$
$$+ \int_{t_0}^{t_f} \{\lambda^{*T}[f(x, u) - \dot{x}]\} \, \mathrm{d}t + l_0^* N[x(t_1), t_1] \tag{43}$$

where ν^*, l_0^*, and $\lambda^*(t)$ denote the constant and time varying multipliers associated with the optimal solution to problem (1–4) and (40). These quantities are not subject to change. Repeating the analysis presented in Sec. II.D, i.e., expanding the augmented cost function about the reference solution, asterisk-indicated and using Eq. (17) to eliminate the $\delta\dot{x}$ term, we arrive, after rearranging, at

$$\mathrm{d}\bar{J} = \left[(\phi + \nu^T \psi)_x - \lambda(t_f)\right] \mathrm{d}x_f + \left[(\phi + \nu^T \psi)_t + H|_{t_f}\right] \mathrm{d}t_f$$
$$+ \int_{t_0}^{t_1} \left[\left(H_x + \dot{\lambda}^T\right)\delta x + H_u \delta u\right] \mathrm{d}t + \int_{t_1}^{t_2} \cdots \, \mathrm{d}t$$
$$+ \left(\lambda^T|_{t_1^+} - \lambda^T|_{t_1^-} + l_0 N_x\right) \mathrm{d}x_1 - \left(H|_{t_1^+} - H|t_1^- - l_0 N_t\right) \mathrm{d}t_1$$
$$+ \lambda^T(t_0) \, \mathrm{d}x_0 - H|_{t_0} \, \mathrm{d}t_0 \tag{44}$$

Note that to perform the integration by parts of the $\delta\dot{x}$ term, it is necessary to break the integral $\int_{t_0}^{t_f}$ at the switching time t_1. Continuity of the integrand across this switching time can not be assumed a priori and, in fact, is not satisfied for all quantities. By choice of λ, ν, and l_0, we find that all coefficients on the right-hand side are zero except for those corresponding to $\mathrm{d}x_0$ and $\mathrm{d}t_0$, and we obtain the same result as in the unconstrained case, namely, $\mathrm{d}\bar{J} = \lambda(t_0) \, \mathrm{d}x_0 - H|_{t_0} \, \mathrm{d}t_0$, Eq. (19). Again, from arguments identical to those used in Sec. II.D. it follows that $\mathrm{d}J = \lambda(t_0)^T \, \mathrm{d}x_0 - H|_{t_0} \, \mathrm{d}t_0$, and $\mathrm{d}J = J^p - J^* + \mathcal{O}^2$, and the numerical procedure for calculating costate approximations as discussed in Secs. II.E and II.F can be applied without modifications.

Using Eq. (41), information about the height of the multiplier jump, represented by the constant multiplier l_0, can be obtained directly from the numerical approximations of the multipliers $\lambda(t)$ just before and just after the jump. This method, however, is not very precise and it can not always be generalized to the case of vector valued interior-point constraints. Difficulties are encountered, for instance, when the Jacobian $\partial N/\partial x|_{t_1}$ has less than full rank. A more efficient method for calculating l_0 is presented in the next section.

C. Relation Between the Multiplier Vector l_0 and Cost Sensitivities

In the present section it is shown that the constant multiplier l_0 represents the sensitivity of the cost function with respect to the constraint (40), in a sense to be specified. Let us consider problem (1–4) subject to the interior point constraint

$$N[x(t_1), t_1] - \alpha_0 = 0 \tag{45}$$

where α_0 is constant. To express the sensitivity of the optimal solution with respect to the parameter α_0 as the sensitivity with respect to a state initial value (the kind of case for which we have derived results in the preceding sections) we augment the dynamical system (2) by

$$\dot{\alpha} = 0, \qquad \alpha(t_0) = \alpha_0 \tag{46}$$

Then the interior-point constraint (40) can be written in the form

$$N[x(t_1), t_1] - \alpha(t_1) = 0, \qquad \alpha(t_1) = 0 \tag{47}$$

Analytically, it is easy to verify that the costate $\lambda_\alpha(t)$ associated with problem (1–4), (46), and (47) satisfies

$$\lambda_\alpha(t) = \begin{cases} -l_0 & \text{for} \quad t < t_1 \\ 0 & \text{for} \quad t > t_1 \end{cases} \tag{48}$$

On the other hand, problem (1–4) (46), and (47) is of the general form of problem (1–4) and (40) discussed in Secs. IV.A and IV.B. Hence, as shown in Secs. IV.A and IV.B, numerical approximations for the costate λ_α can be obtained by applying the methods of Secs. II.E and II.F. Through Eq. (48), this immediately provides a method for calculating the multiplier l_0. From Eq. (48) it is also clear that l_0 represents the sensitivity of the optimal cost with respect to the prescribed value of the constraint function $N[x(t_1), t_1]$.

V. State Constrained Problems

A. Problem Formulation and Optimality Conditions

For simplicity, let us consider only a scalar state inequality constraint. The generalization to vector valued state constraints is then straightforward. A method for treating state equality constraints is not immediately obvious but becomes clear from the subsequent sections dealing with the costate calculation along arcs where the state inequality constraint is active.

Hence, in this section we consider problem (1–4) subject to a scalar state inequality constraint of the form

$$g(x, t) \le 0 \tag{49}$$

Assume that the optimal switching structure for problem (1–4) and (49) is

$$g(x,t) \begin{cases} <0 & \text{on} \quad [t_0, t_1) \\ =0 & \text{on} \quad [t_1, t_2] \\ <0 & \text{on} \quad (t_2, t_f] \end{cases} \tag{50}$$

The generalization of the following analysis to any other switching structure is straightforward as long as the state constraint is nonactive along the first arc.

Following a standard procedure for analyzing state constrained arcs, the condition

$$g(x, t) = 0 \qquad \forall t \in [t_1, t_2], \qquad t_1 > t_2 \tag{51}$$

is divided equivalently into a set of interior point constraints and a control constraint (on $[t_1, t_2]$), namely,

$$\begin{aligned} g(x,t)|_{t_1} &= 0 \\ \left.\frac{\mathrm{d}g(x,t)}{\mathrm{d}t}\right|_{t_1} &= 0 \\ &\vdots \\ \left.\frac{\mathrm{d}^{q-1}g(x,t)}{\mathrm{d}t^{q-1}}\right|_{t_1} &= 0 \end{aligned} \tag{52}$$

and

$$\frac{\mathrm{d}^q g(x,t)}{\mathrm{d}t^q} = 0 \quad \forall t \in [t_1, t_2] \tag{53}$$

Here, q is the smallest integer i for which a control u appears explicitly in $\mathrm{d}^i g(x,t)/\mathrm{d}t^i$ and is called the order of the state constraint. Define

$$N[x(t_1), t_1] = \begin{bmatrix} g(x,t)|_{t_1} \\ \left.\frac{\mathrm{d}g(x,t)}{\mathrm{d}t}\right|_{t_1} \\ \vdots \\ \left.\frac{\mathrm{d}^{q-1}g(x,t)}{\mathrm{d}t^{q-1}}\right|_{t_1} \end{bmatrix} \tag{54}$$

and

$$c(x, u, t) = \frac{\mathrm{d}^q g(x,t)}{\mathrm{d}t^q} \tag{55}$$

Along subarcs of the optimal solution to problem (1–4) and (49), where the state inequality constraint (49) is satisfied with strict inequality the optimality conditions presented in Eqs. (5–13) are satisfied and the solution behaves as if the constraint (49) were deleted. Along the subarc $[t_1, t_2]$ of the optimal solution, throughout which $g(x,t) = 0$, the optimal control $u(t)$, the multiplier $\mu(t)$, and the costate differential equation are determined through conditions (33–36) with $c(x, u, t)$ defined by Eq. (55). Note that the condition (34) only guarantees that the qth derivative of the state constraint (49) is equal zero. To ensure that $g(x,t) = 0$ is satisfied along the constrained arc, the conditions

$$N[x(t_1), t_1] = 0 \tag{56}$$

have to be enforced, $N[x(t_1), t_1]$ as in Eq. (54). Similarly to conditions (41) and (42) for scalar interior point constraints, the condition (56) causes a discontinuous jump in the Lagrange multipliers $\lambda(t)$ and in the Hamiltonian H, namely,

$$\lambda(t_1^+)^T = \lambda(t_1^-)^T - l^T \frac{\partial N[x(t_1), t_1]}{\partial x(t_1)} \tag{57}$$

$$H|_{t_1^+} = H|_{t_1^-} + l^T \frac{\partial N[x(t_1), t_1]}{\partial t_1} \tag{58}$$

Here, $l^T = [l_0, \dots, l_{q-1}]$ is a q-dimensional vector of constant multipliers that compensates for the q degrees of freedom lost by enforcing the conditions (54). At the exit time t_2 of the constrained arc the Lagrange multipliers and the Hamiltonian have to be continuous, i.e.,

$$\lambda(t_2^+) = \lambda(t_2^-) \tag{59}$$

$$H|_{t_1^+} = H|_{t_1^-} \tag{60}$$

B. Relation Between the Lagrange Multipliers $\lambda(t)$ and Cost Sensitivities Along Unconstrained Arcs

In this section we assume again that the optimal switching structure to problem (1–4) and (49) is as shown in Eq. (50). A generalization to other switching structures will be straightforward as long as the trajectory starts with an unconstrained arc.

From the equivalence of Eq. (51) and Eqs. (52) and (53), it is clear that an active state constraint can be considered as a combination of an interior-point constraint and a control constraint. From the analyses presented in Secs. III and IV it is hence clear that we should start our present investigation with an augmented cost function of the form

$$\bar{J} = \phi[x(t_f), t_f] + \nu^{*T}\psi[x(t_f), t_f] + \int_{t_0}^{t_f} [\lambda^{*T}(f(x,u) - \dot{x}) + \mu^{*T} c(x,u,t)]\,\mathrm{d}t + l^{*T} N[x(t_1), t_1] \tag{61}$$

where ν^*, l^*, $\lambda^*(t)$, and $\mu^*(t)$ denote the constant and time varying multipliers associated with the optimal solution to problem (1–4) and (49) and are not subject to change in the following analysis. In complete analogy to the analyses presented in Secs. II.D, III.B, and IV.B, we arrive at the following expression for the first variation of the augmented cost function (61) (again, the superscript asterisks are dropped for convenience):

$$\begin{aligned}\mathrm{d}\bar{J} &= \left[(\phi + \nu^T\psi)_x - \lambda(t_f)\right]\mathrm{d}x_f + \left[(\phi + \nu^T\psi)_t + H|_{t_f}\right]\mathrm{d}t_f \\ &+ \int_{t_0}^{t_1} \left[\left(H_x + \mu c_x + \dot{\lambda}^T\right)\delta x + (H_u + \mu c_u)\delta u\right]\mathrm{d}t \\ &+ \int_{t_1}^{t_2} \cdots\,\mathrm{d}t + \int_{t_2}^{t_f} \cdots\,\mathrm{d}t + \left(\lambda^T|_{t_1^+} - \lambda^T|_{t_1^-} + l^T N_x\right)\mathrm{d}x_1 \\ &+ \left(\lambda^T|_{t_2^+} - \lambda^T|_{t_2^-}\right)\mathrm{d}x_2 + \left(H|_{t_1^+} - H|_{t_1^-} + l^T N_t\right)\mathrm{d}t_1 \\ &+ \left(H|_{t_2^+} - H|_{t_2^-}\right)\mathrm{d}t_2 + \lambda^T(t_0)\,\mathrm{d}x_0 - H|_{t_0}\,\mathrm{d}t_0\end{aligned} \tag{62}$$

By choice of λ, μ, ν, and l, we find that all terms on the right-hand side are zero except for those involving $\mathrm{d}x_0$ and $\mathrm{d}t_0$ and we obtain the same result, Eq. (19), as before in Secs. II.D, III.B, and IV.B, namely, $\mathrm{d}\bar{J} = \lambda(t_0)\,\mathrm{d}x_0 - H|_{t_0}\mathrm{d}t_0$. Again, through arguments identical to those used in Sec. II.D, this result implies that $\mathrm{d}J = \lambda(t_0)^T\,\mathrm{d}x_0 - H|_{t_0}\mathrm{d}t_0$. From $\mathrm{d}J = J^p - J^* + \mathcal{O}^2$, it follows again that the left-hand side of this equation can be approximated by finite differences, and the numerical procedure for calculating costate approximations as discussed in Secs. II.E and II.F can be applied without modifications.

As a caution it should be noted, however, that it was assumed in the present section that the solution starts with an unconstrained arc. In applying the numerical procedure of Sec. II.F for the automatic costate calculation in the interior of the optimal trajectory, this translates into the assumption that the current time at which a costate is being calculated lies on an unconstrained arc. A generalization to the case where the Lagrange multiplier vector is being sought at an instant of time along a constrained arc is not quite obvious. Note that in such a case certain state perturbations are not admissible as they would lead to a violation in the state constraint (49). A precise treatment of this case will be given in the subsequent sections.

C. Relation Between the Lagrange Multipliers $\lambda(t)$ and Cost Sensitivities Along Constrained Arcs

In this section we consider the case where the optimal switching structure for the solution to problem (1–4) and (49) is of the form

$$g(x,t)\begin{cases} =0 & \text{on} \quad [t_0, t_1] \\ <0 & \text{on} \quad (t_1, t_f] \end{cases} \tag{63}$$

Generalization of the following analysis to any other switching structure that starts with a constrained arc is straightforward. The difficulty associated with the calculation of the Lagrange multiplier vector at time t_0 in this case is that different results are obtained depending on whether t_0 is considered the end of an (infinitesimally short) unconstrained arc or the beginning of a constrained arc. These differences are associated with the multiplier jump (57) at switching points from unconstrained to constrained arcs.

If we consider t_0 as the end point of an infinitesimally short unconstrained arc, then the analysis of the preceding section is applicable without changes and the same result (19) is obtained. Additional care has to be taken only during the numerical implementation of the schemes discussed in Secs. II.E and II.F. All perturbations (22) and (23) have to be chosen such that the state constraint (49) remains satisfied at the perturbed initial states and time, i.e.,

$$g\left[x^i\left(t_0^i\right), t_0^i\right] \leq 0, \qquad i = 1, \ldots, n+1 \tag{64}$$

for all $x^i(t_0^i)$, with t_0^i as in Eq. (21). Clearly, for a scalar state constraint $g(x,t) \leq 0$ that is active at t_0, there are at most n linearly independent perturbations in initial time and initial states such that g remains zero at t_0, and at least one out of the $n+1$ perturbations required to perform the multiplier calculation discussed in the preceding section leads to $g(x,t) < 0$. The associated perturbed solution then starts with a (short) unconstrained arc of nonzero length.

To calculate the Lagrange multipliers in the interior of a constrained arc (in this case t_0 is considered the beginning of a constrained arc) one can simply add the multiplier jump (57) to the results obtained earlier for the Lagrange multiplier at the end of an infinitesimally short unconstrained arc. This requires explicit knowledge of the constant multiplier vector $\boldsymbol{l} \in \boldsymbol{R}^q$. A numerical method for calculating l can be developed in the style of Sec. IV.C. This is discussed in more detail in the next section.

It is interesting to note that another, more direct method for the calculation of $\lambda(t_0^+)$ [the value of $\lambda(t_0)$ at the beginning of the constrained arc] can be developed by exploiting the equivalence of condition (51) and conditions (52) and (53). By enforcing initial states such that the conditions (52) (with t_1 replaced by t_0) are satisfied automatically, the jump onto the state constraint (49) is performed implicitly through the problem formulation and satisfaction of the state constraint $g(x,t) = 0$ on $[t_0, t_1]$ can be enforced through the control constraint (53) (with t_1 and t_2 replaced by t_0 and t_1, respectively).

Explicitly, let $\xi \in \boldsymbol{R}^n$ denote the initial state of the optimal solution to problem (1–4) and (49), i.e.,

$$\xi = x^*(t_0) \tag{65}$$

Then define an auxiliary problem through conditions (1), (2), and (4), the initial conditions

$$x(t_0) = \xi \tag{66}$$

and the control constraint

$$c(x,u,t) \leq 0 \tag{67}$$

where c is as defined in Eq. (55). Clearly, this auxiliary problem represents a control-constrained problem of the general form discussed in Sec. III. The result (19) obtained in Sec. III.B can be easily shown to hold also for the switching structure (63) with $g(x,t)$ replaced by $c(x,u,t)$. {Here and in Eq. (67), it is tacitly assumed that the optimal solution to the state constrained problem (1–4) and (49) satisfies $c(x,u,t) = 0$ on $[t_0, t_1]$, $c(x,u,t) < 0$ on $(t_1, t_f]$. An extension of the results obtained in this section to the case where the state constraint becomes active a second time (or even more times) is straightforward but involves some tedious bookkeeping.} Hence, a method for calculating the costate value $\lambda(t_0^+)$ for the state constrained problem (1–4) and (49) is obtained by applying the numerical scheme of Secs. II.E and II.F to the control-constrained problem (1), (2), (4), (66), and (67). It should be noted that this scheme requires the explicit differentiation of the constraint function $g(x,t)$ to determine the functions $N(x,t)$ and $c(x,u,t)$ defined in Eqs. (54) and (55).

D. Relation Between the Multiplier Vector l and Cost Sensitivities

To outline a method for the automatic calculation of the constant multiplier vector $\boldsymbol{l} \in \boldsymbol{R}^q$ associated with problem (1–4) and (49), we assume again that the optimal solution has the switching structure (50). A generalization to other switching structures is straightforward as long as the optimal solution starts with an unconstrained arc. In this context, solutions that start with a constrained arc can be viewed as starting with an infinitesimally short unconstrained arc.

We now consider problem (1–4) subject to the state constraint

$$g(x,t) - \sum_{i=0}^{q-1} \frac{\beta_i}{i!}\left(t - t_1^*\right)^i \le 0 \tag{68}$$

where t_1^* denotes the optimal switching time t_1 associated with the solution to problem (1–4) and (49). For all $\beta \in \boldsymbol{R}^q$, Eq. (68) represents a qth-order state inequality constraint, and for

$$\beta_i = 0, \qquad i = 0,\ldots,q-1 \tag{69}$$

Equation (68) reduces to Eq. (49). We assume that for all β values within some neighborhood of Eq. (69), the optimal solution of Eqs. (1–4) and (68) has the switching structure (50). (Otherwise, constraint (68) has to be changed appropriately along the intervals $[t_0, t_1)$ and $(t_2, t_f]$.) Then Eq. (68) can be divided equivalently into the interior point constraint

$$N[x(t_1), t_1] = \beta \tag{70}$$

and the control constraint on $[t_1, t_2]$,

$$c(x, u, t) = 0 \tag{71}$$

where N and c are as in Eqs. (54) and (55), respectively. To raise the status of the parameters $\beta_0, \ldots, \beta_{q-1}$ to that of states, we augment the problem (1–4) and (68) through the state equations

$$\begin{aligned} \dot{b}_0 &= 0 \\ &\vdots \\ \dot{b}_{q-1} &= 0 \end{aligned} \tag{72}$$

and the initial conditions

$$\begin{aligned} b_0(t_0) &= \beta_0 \\ &\vdots \\ b_{q-1}(t_0) &= \beta_{q-1} \end{aligned} \tag{73}$$

Then the state constraint (68) can be written in the form

$$g(x,t) - \sum_{i=0}^{q-1} \frac{b_i(t_1)}{i!}\left(t - t_1^*\right)^i \le 0 \tag{74}$$

Clearly, for β given by Eq. (69), problem (1–4) and (68) is identical to problem (1–4) and (49). Hence the optimal solution x^* to problem (1–4) and (72–74) is identical to the optimal solution to problem (1–4) and (49). Careful examination of the necessary conditions for optimality shows that in this case also the costates λ_x and the multipliers $\boldsymbol{l} \in \boldsymbol{R}^q$ are identical for both problems. Hence, to calculate the multiplier vector $\boldsymbol{l} \in \boldsymbol{R}^q$ associated with problem (1–4) and (72–74), it suffices to calculate the multiplier vector $\boldsymbol{l}$ associated with problem (1–4) and (72–74). We note that for the latter problem the adjoint equations, transversality conditions, and jump conditions for the costate vector $\boldsymbol{\lambda}_a$ are given by

$$\begin{aligned} \dot{\boldsymbol{\lambda}}_a &= 0 \\ \boldsymbol{\lambda}_a(t_f) &= 0 \\ \boldsymbol{\lambda}_a\left(t_1^+\right) &= \boldsymbol{\lambda}_a\left(t_1^-\right) + \boldsymbol{l} \end{aligned} \tag{75}$$

This system can be integrated analytically to yield

$$\boldsymbol{\lambda}_a(t) = \begin{cases} -\boldsymbol{l} & \text{on} \quad [t_0, t_1) \\ 0 & \text{on} \quad (t_1, t_f] \end{cases} \tag{76}$$

In particular, we find

$$\boldsymbol{l} = -\boldsymbol{\lambda}_a(t_0) \tag{77}$$

Hence, to determine $\boldsymbol{l}$, we can equivalently calculate $\boldsymbol{\lambda}_a(t_0)$. For this task we can apply the numerical methods presented in Secs. II.E and II.F.

Another helpful analytical relation that can be proven easily for problem (1–4) and (49) is

$$l_0 = \mu(t_1) \tag{78}$$

Here it is again assumed that the optimal switching structure is given by Eq. (50), and $\mu(t)$ denotes the scalar multiplier function of time introduced through the Kuhn–Tucker conditions (33–35).

If costate values are calculated for a sequence of initial times and initial states that are marching along the reference solution in the style described in Sec. II.F, then different values for $\boldsymbol{l}$ are obtained depending on what time along the original reference solution is chosen as the new initial time. Let $\boldsymbol{L}(t)$ denote the so-obtained value of $\boldsymbol{l}$ as a function of the initial time t. Along the interval $[t_0, t_1]$, the components of $\boldsymbol{L}(t)$ stay constant and equal to the optimal multiplier vector $\boldsymbol{l}$ associated with the original problem (1–4) and (49). Along $[t_2, t_f]$, all components of $\boldsymbol{L}(t)$ stay equal zero, reflecting the fact that the state constraint (68) and (69) is inactive for all times greater than the current initial time, so that the cost sensitivity is zero with respect to all components of β. On the interval $[t_1, t_2]$, function $\boldsymbol{L}(t)$ changes with the initial time t, in general, and, through Eq. (78), the first component $L_0(t)$ of the vector function $\boldsymbol{L}(t)$ provides the value of $\mu(t)$ on the interval $[t_1, t_2]$. In summary, from the analysis we find that

$$L_0(t) = \begin{cases} l_0 & \text{on} \quad [t_0, t_1] \\ \mu(t) & \text{on} \quad [t_1, t_2] \end{cases} \tag{79}$$

VI. Numerical Implementation and Results

A. Direct Optimization Approach

As a central element the schemes for automatic costate calculation presented in this paper rely on a numerical method for calculating near-optimal state histories. The numerical results presented here are generated using the software package Trajectory Optimization via Differential Inclusion (TODI).[11] The underlying optimization method resembles a collocation approach, however, it is based on a differential inclusion representation for the dynamical system that leads to the elimination of all control variables from the optimization process. In principle, any other optimization code is applicable. Because of its robust convergence behavior, however, this method seems to be well suited to perform the recurrent calculation of reference solutions and perturbed solutions in unsupervised do-loops without user intervention.

TODI generates approximations to the optimal states at a user chosen grid along the time axis of, say, N nodes. A first iterate of the Lagrange multipliers $\lambda(t)$ at these nodes is calculated based on the analysis of Sec. II designed for arcs along which no constraints are active. Then the correct value of the Lagrange multiplier $\lambda(t)$ along the arc with active state constraint is obtained by performing the multiplier jump (57). The constant multiplier vector $\boldsymbol{l}$ that has to be known to perform this step is calculated simultaneously with λ^{free}, based on the analysis presented in Sec. V.

B. Numerical Example: State Constrained Brachistochrone Problem

Consider the problem

$$\min_{u \in PWC[t_0, t_f]} t_f \tag{80}$$

subject to the equations of motion

$$\begin{aligned} \dot{x}(t) &= v(y)\,\cos\theta(t) \\ \dot{y}(t) &= v(y)\,\sin\theta(t) \end{aligned} \tag{81}$$

the boundary conditions

$$\begin{aligned} x(0) &= 0, \qquad & x(t_f) &= 1 \\ y(0) &= 0, \qquad & y(t_f) &\ \text{free} \end{aligned} \tag{82}$$

and the state constraint

$$y(t) - x(t)\,\tan\gamma - h_0 \le 0 \tag{83}$$

Here, x and y are the state variables and θ is the only control. The quantity v denotes the velocity and is a short notation for $v = \sqrt{(v_0^2 + 2gy)}$. The quantities v_0, g, γ, and h_0 are constant. For numerical calculations we use

$$v_0 = 1, \qquad g = 1, \qquad \gamma = 20, \qquad h_0 = 0.05 \tag{84}$$

The state inequality constraint (83) being active along some nonzero time interval $[t_1, t_2] \subseteq [t_0, t_f]$ is equivalent to

$$y(t_1) - x(t_1)\tan\gamma - h_0 = 0 \tag{85}$$

and on $[t_1, t_2]$,

$$\sin\theta(t) - \cos\theta(t)\tan\gamma \equiv 0 \tag{86}$$

The left-hand sides of Eqs. (85) and (86) can be identified as N and c in the general formulation presented in Sec. V.A and the state constraint (83) is of order $q = 1$. Hence, for the present problem, the multiplier vector $\boldsymbol{l} \in \boldsymbol{R}^q$ introduced in Eqs. (57) and (58) is a scalar and will henceforth be denoted by l_0.

Following the general formulation presented in Secs. II.B and V.A, we obtain the costate equations

$$\begin{aligned} \dot{\lambda}_x &= 0 \\ \dot{\lambda}_y &= -\lambda_x(g/v)\cos\theta - \lambda_y(g/v)\sin\theta \end{aligned} \tag{87}$$

These equations hold (for the present problem) in the same form for free arcs and for constrained arcs.

Along unconstrained arcs the conditions (12) and (13) imply

$$\begin{bmatrix} \sin\theta \\ \cos\theta \end{bmatrix} = -\begin{bmatrix} \lambda_y \\ \lambda_x \end{bmatrix} \frac{1}{\sqrt{\lambda_x^2 + \lambda_y^2}} \tag{88}$$

and

$$\mu = 0 \tag{89}$$

Along constrained arcs, the optimal control $\theta(t)$ and the multiplier function of time $\mu(t)$ determined through the Kuhn–Tucker conditions (33–35) are

$$\theta = \gamma \tag{90}$$

$$\mu = (\lambda_x \sin\gamma - \lambda_y \cos\gamma)\cos\gamma \tag{91}$$

The jump conditions (57) and (58) take the explicit form

$$\begin{aligned} \lambda_x\left(t_1^+\right) &= \lambda_x\left(t_1^-\right) + l_0 \cdot \tan\gamma \\ \lambda_y\left(t_1^+\right) &= \lambda_y\left(t_1^-\right) - l_0 \cdot 1 \end{aligned} \tag{92}$$

$$H|_{t_1^+} - H|_{t_1^-} = 0 \tag{93}$$

Here

$$H = \lambda_x v\cos\theta + \lambda_y v\sin\theta \tag{94}$$

denotes the Hamiltonian defined in Eq. (10). The transversality conditions (6–8) can be reduced to the simple form

$$\lambda_y(t_f) = 0 \tag{95}$$

$$H|_{t_f} = -1 \tag{96}$$

through analytical elimination of the constant multiplier vectors ν_0 and ν_f.

With respect to the state constraint (83), the optimal solution to problem (80–84) has the switching structure

$$\text{free—constrained—free} \tag{97}$$

In general, the switching structure has to be determined through numerical experiments using a trial and error approach. The associated optimality conditions yield a MPBVP that is solved numerically using a shooting method.[6–8] The numerical solution of this MPBVP is referred to as the exact optimal solution henceforth and is used as a truth model for comparison with the suboptimal solutions obtained with TODI through parameter optimization. In Figs. 1–6 the exact optimal time histories of the states x and y, the costates λ_x and λ_y, the constraint $c = y - x\tan\gamma - h_0$, and the multiplier μ, respectively, are represented as solid lines.

For the TODI approach a node density of 101 nodes is chosen. As initial guesses

$$t_f = 1 \tag{98}$$

is used and all states are set equal zero throughout the 101 nodes, i.e.,

$$x_i^j = 0, \qquad i = 1, \ldots, n, \qquad j = 1, \ldots, 101 \tag{99}$$

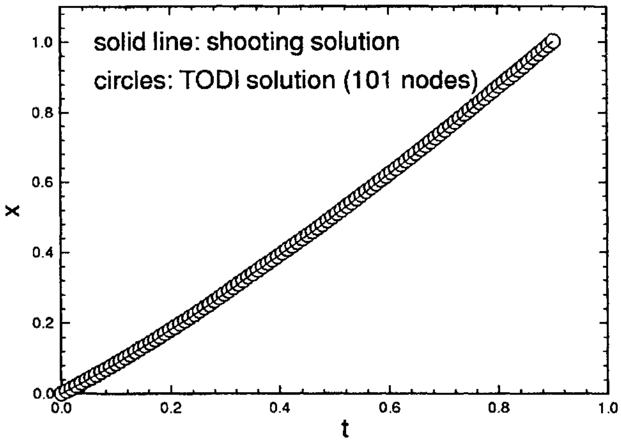

Fig. 1 State x vs time t.

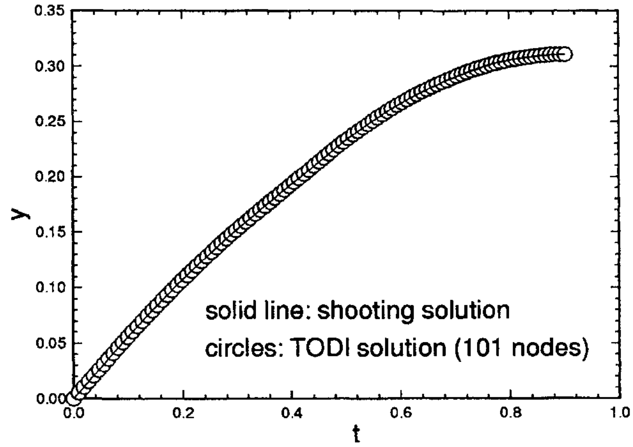

Fig. 2 State y vs time t.

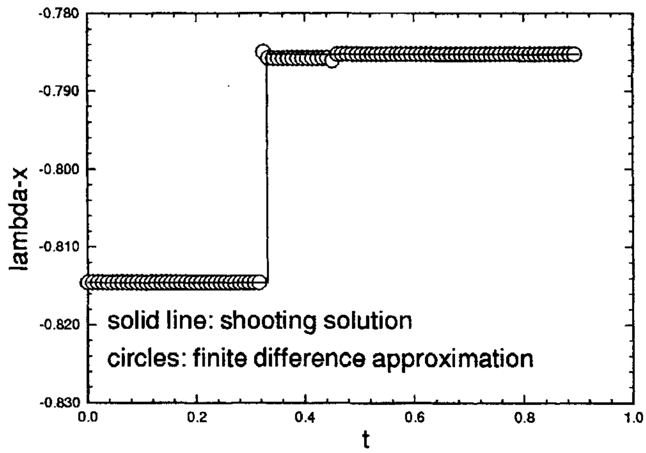

Fig. 3 Costate λ_x vs time t.

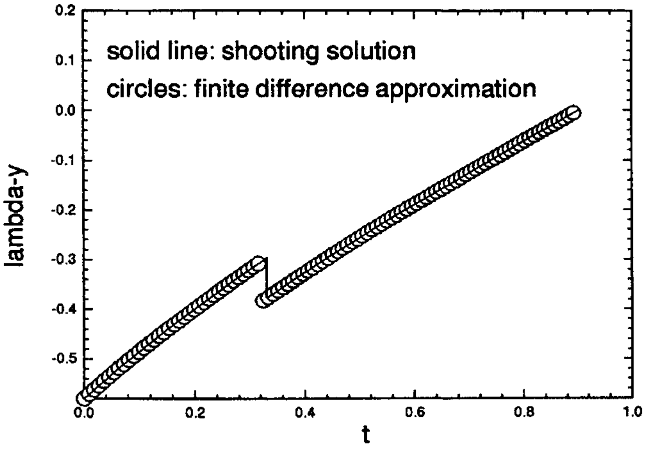

Fig. 4 Costate λ_y vs time t.

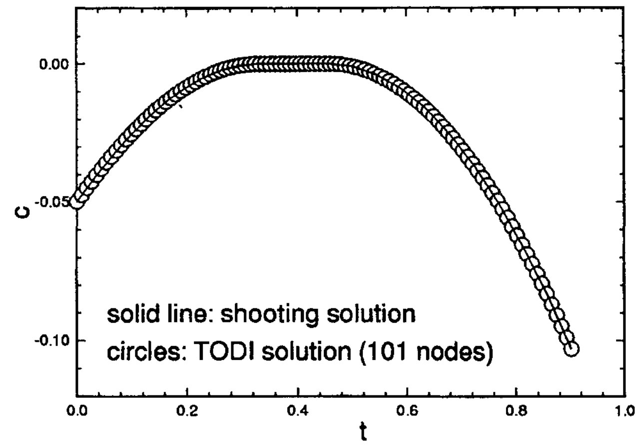

Fig. 5 Constraint c vs time t.

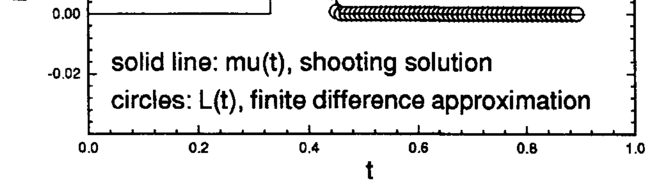

Fig. 6 Multiplier μ and function L (defined in Sec. II.E) vs time t.

A guess for the switching structure does not have to be provided. The near-optimal solutions for states x and y and the constraint c at the 101 nodes is represented by circles in Figs. 1, 2, and 5 and is seen to coincide well with the optimal variational solution.

Once the parameter optimal solution is obtained, it is frozen and kept as the reference solution about which perturbed solutions are generated as required by the analyses of Secs. II.E and II.F. The obtained approximations for the Lagrange multipliers λ_x and λ_y are shown in Figs. 3 and 4. In Fig. 6, the function $L_0(t)$ introduced in Sec. V.D is superimposed with the multiplier function of time $\mu(t)$. The significance of $L_0(t)$ is summarized in Eq. (79), and the agreement with $\mu(t)$ on the interval $[t_1, t_f]$ is seen to be excellent.

It is important to note that user provided initial guesses are required only to generate the approximate state histories (indicated by circles in Figs. 1 and 2). All other results are obtained simply by running programs without user supervision.

VII. Summary and Conclusions

A finite difference approach for the automatic calculation of costates is presented. The method exploits the relation between the costates and certain sensitivities of the cost function. The complete theoretical background for treating free, control-constrained, interior-point-constrained, and state-constrained optimal control problems is presented. The numerical implementation relies on the calculation of near optimal trajectories. In the present paper a differential inclusion based approach is employed for this task. In principle, however, any other direct optimization approach is applicable.

As a numerical example a state constrained Brachistochrone problem is solved, and the results are compared with the optimal solution obtained from a shooting method. The agreement is found to be excellent.

Acknowledgment

This work was supported by NASA Langley Research Center under Contract NAS1-20131.

References

[1] Pontryagin, L. S., Boltyanskii, V. G., Gamkrelidze, R. V., and Mischemko, E. F., *The Mathematical Theory of Mathematical Processes*, Interscience, New York, 1962.

[2] Bryson, A. E., and Ho, Y. C., *Applied Optimal Control*, Hemisphere, New York, 1975.

[3] Lee, E. B., and Markus, L., *Foundations of Optimal Control Theory*, Krieger, Malabar, FL, 1986.

[4] Leitmann, G., *The Calculus of Variations and Optimal Control*, Plenum, New York, 1981.

[5] Neustadt, L. W., *Optimization: A Theory of Necessary Conditions*, Princeton Univ. Press, Princeton, NJ, 1976.

[6] Roberts, S. M., and Shipman, J. S., *Two-Point Boundary Value Problems: Shooting Methods*, American Elsevier, New York, 1972.

[7] Roberts, S. M., and Shipman, J. S., "Multipoint Solution of Two-Point Boundary Value Problems," *Journal of Optimization Theory and Applications*, Vol. 6, No. 4, 1971, pp. 301–318.

[8] Stoer, J., and Bulirsch, R., *Introduction to Numerical Analysis*, English translation by R. Bartles, W. Gautschi, and C. Witzgall, Springer–Verlag, New York, 1980.

[9] Wouk, A., *A Course of Applied Functional Analysis*, Wiley, New York, 1979.

[10] Gill, P. E., Murray, W., and Wright, M. H., *Practical Optimization*, Academic, New York, 1981.

[11] Seywald, H., "Trajectory Optimization Based on Differential Inclusion," *Journal of Guidance, Control, and Dynamics*, Vol. 17, No. 3, 1994, pp. 480–487.

[12] Enright, P. J., and Conway, B. A., "Discrete Approximations to Optimal Trajectories Using Direct Transcription and Nonlinear Programming," AIAA Paper 90-2963, 1990.

[13] Martell, C. A., and Lawton, J. A., "Adjoint Variable Solutions via an Auxiliary Optimization Problem," *Journal of Guidance, Control, and Dynamics*, Vol. 18, No. 6, 1995, pp. 1267–1272.

[14] von Stryck, O., "Numerical Solution of Optimal Control Problems by Direct Collocation," *Optimal Control*, edited by R. Bulirsch, A. Miele, J. Stoer, and K. H. Well, Vol. 111, International Series of Numerical Mathematics, Birkhäuser Verlag, Basel, Switzerland, 1993.

[15] Ewing, G. M., *Calculus of Variations*, Dover, New York, 1985.